# Drastic suppression of scattering and activated behavior in mesoscopic quantum Hall systems with smooth confinement

O. G. Balev
*Institute of Physics of Semiconductors, National Academy of Sciences, 45 Prospekt Nauky, Kiev 252650, Ukraine*

P. Vasilopoulos
*Concordia University, Department of Physics, 1455 de Maisonneuve Boulevard O, Montréal, Québec, Canada, H3G 1M8*
(Received 9 May 1994)

It is shown that in a degenerate two-dimensional electron gas (2DEG), *intralevel intracenter* electron transitions due to a strong impurity potential, for not too low temperatures, can lead to the observed activated behavior of the resistivity in micrometer- or submicrometer-width parabolic channels. This contribution is exponentially suppressed if the Fermi level is not too close to the bottom of the nearest Landau level. As the temperature decreases, at fixed confining potential, this activated behavior is changed to a temperature-independent behavior that is usual for elastic scattering of the degenerate 2DEG. The latter is related with *intralevel interedge* electron transitions. The asymmetry of the Shubnikov–de Haas oscillations and their dependence on confinement and temperature are obtained in agreement with experimental observations.

## I. INTRODUCTION

Dissipation processes in electron transport related with edge states in mesoscopic quantum Hall systems[1] have attracted considerable attention especially after the publication of Ref. 2. These processes were studied in many recent theoretical and experimental papers; see, e.g., Refs. 3–12 and the review of Ref. 13. Recently, some investigations, Refs. 14 and 15, that give a spreading out of the current density, indicate that additional treatments of dissipation are necessary in narrow channels. In a GaAs/(AlAs)Ga heterostructure,[14] an almost linear spatial dependence of the Hall potential was observed for current densities $j_x \approx 0.01$ A/m; this is rather different than its behavior for $j_x$ about four times smaller[14] (for $j_x \leq 0.0025$ A/m the spatial behavior of the Hall potential is almost independent of $|j_x|$ ). In Ref. 15 a substantial sharing of the total net current, between edge and bulk states, is obtained in the linear regime for hard-wall confinement which contributes mostly to the edge current. Thus for smooth confining potentials the bulk current contribution to the total current along the Hall bar should be larger[15] than that for hard-wall confinement. A smooth confining potential is now considered as a more realistic model[9,12,16–21] for describing many experimental observations in two-dimensional electron gas (2DEG) channels. However, the frequency[18,19] $\Omega$ of the confining potential and the typical scale at which it changes at the edges of the channel $y_e$, are still not well known (cf. Refs. 9, 12, and 16–21). Some theoretical results[20] lend support to the estimate $y_e \approx 0.5$ $\mu$m made in Refs. 16 and 17. Assuming a spreading out of the current density, we will take into account the Hall field $E_H$ in the manner of Ref. 19.

We will study the dissipation in the linear regime of the quantum Hall effect (QHE) in a narrow channel, of infinite length, in the presence of a strong perpendicular magnetic field $B$ such that $\hbar\omega_c \gg k_BT$, where $\omega_c = |e|B/m^*$ is the cyclotron frequency, $m^*$ the effective mass, and $e$ ($< 0$) the electron charge. We will consider electron scattering by a random static potential as well as by acoustical phonons. The applied electric fields (along the channel) are supposed to satisfy the condition $|E_x/E_H| \ll 1$ due to the strong magnetic field. Spin splitting is neglected unless otherwise stated. We will study both *intralevel* and *interlevel* transitions for elastic and inelastic scattering. In Ref. 3 these transitions were studied only for inelastic scattering and the result was[3] that there is no exponential suppression, compare Ref. 10. In Ref. 11 only interlevel transitions were treated for strong confinement, with a typical group velocity of an edge state $v_g \approx 10^7$ cm/s. However, we have obtained an exponential suppression of the *intralevel* contribution to the dissipation for typical scattering processes due to acoustical phonons at the edges,[21] when the confinement is smooth, i.e., when the typical $v_g$ of an edge state is smaller than the speed of sound $s$, $v_g \lesssim 10^5$ cm/s for a GaAs/(AlGa)As heterostructure. For $v_g \geq s$ we have no exponential suppression of the dissipation[19,21] for linear responses and finite $E_H$ (or $j_x$). The strong *intralevel* inelastic scattering in Ref. 3 can be ascribed to an assumed rather strong confinement that leads to the estimate $v_g \approx 10^7$ cm/s. Notice that in Refs. 18 and 21 a much smaller $v_g$ is estimated: for $B = 3.9$ T. Ref. 18 finds $v_g \approx E_H/B = 10^6$ cm/s with $\Omega = 7.8 \times 10^{11}$ s$^{-1}$. The treatments of Refs. 20 and 21 show that in some rather

 

typical experiments smoother confinements are possible at least for edge states near the Fermi level, in agreement with Refs. 16 and 17. Here we show that in the linear regime the dissipation due to *intralevel* impurity scattering, is exponentially suppressed for smooth confining potentials if the Fermi level is not too close to the bottom of the Landau level. Moreover, for a degenerate 2DEG this exponentially suppressed dissipation can be temperature independent but for smaller $\Omega$ it can be activated. The former behavior is related with *intralevel interedge* transitions of electrons with coordinates $|y| \approx W/2$, within the same Landau level. The latter behavior is related with impurity assisted *intralevel intracenter* transitions involving electron coordinates $|y| \ll W/2$.

In addition, we obtain the asymmetry in the Shubnikov–de Haas oscillations and the dependence of the latter on $\Omega$ and $T$. The resistivity at the low-energy side of the Landau level is substantially smaller than at its high-energy side if $T$ is not too high and $\Omega$ not too small. Moreover, we study dissipation due to *intralevel intraedge* electron transitions. Such transitions should be possible in an experiment due to the nonequilibrium population of the edge states that results from nonequilibrium processes at the current probes[2,7] and/or an energy-dependent rate of the transitions between interlevel edge states.[9]

The paper is organized as follows. In Sec. II we present, for convenience, some basic relations from Ref. 19 appropriately modified to take into account the interaction with phonons and a static random potential. In Sec. III we calculate the dissipation in a narrow channel due to interaction with impurities for intralevel and interlevel transitions; in Sec. IV we do the same for transitions assisted by acoustical phonons. Finally, in Sec. V we present the concluding remarks.

## II. BASIC RELATIONS: CHANNEL CHARACTERISTICS

We consider a 2DEG confined in a narrow channel, in the $(x,y)$ plane, of width $W$, length $L_x = L$, and of finite thickness $L_z = d$. The width $W$ is smaller or much smaller than the size of the sample $L_y$ in the $y$ direction, see below. For $W \lesssim 0.1$ $\mu$m we can take the confining potential as parabolic: $V_y = m^*\Omega^2 y^2/2$; here intralevel interedge, intralevel intraedge, and interlevel intraedge electron transitions can be important. However, the results related with intralevel intraedge and interlevel intraedge electron transitions can be directly extended to the case of the more realistic potential $V_y' = 0$ for $y_l < y < y_r$, $V_y' = m^*\Omega^2(y-y_r)^2/2$ for $y > y_r > 0$, and $V_y' = m^*\Omega^2(y-y_l)^2/2$ for $y < y_l < 0$ , for $W \gtrsim 1$ $\mu$m, see Ref. 19. In the latter case, for $W > 1$ $\mu$m, we have $W \approx y_r - y_l$. For definiteness, in what follows we will consider $V_y$ . For the confinement in the $z$ direction we normally assume $d = 0$; otherwise we consider a parabolic well of frequency $\omega_z$ or the standard triangular well. Now as explained in Ref. 19, when a weak electric field $E_x$ is applied along the channel and a strong magnetic field $B$ along the $z$ axis, we should include the Hall field $E_H$ in the Hamiltonian. Then the current density, averaged over a statistical ensemble and the dimensions of the channel, reads

$$j_y = \sigma_{yy}(E_H)E_H + \sigma^0_{yx}E_x = 0, \tag{1}$$

$$j_x \approx \sigma^0_{xy}E_H. \tag{2}$$

Here $\sigma^0_{yx} = -\sigma^0_{xy} \propto e^2/2\pi\hbar$ is the conductivity in the absence of any interaction. The first term on the right-hand side of Eq. (1), $j_d = \sigma_{yy}(E_H)E_H = j^i_d + j^p_d$, expresses dissipation due to the interaction with impurities ($j^i_d$) and phonons ($j^p_d$). With $[\vec{q} = (\vec{q}_\perp, q_z)$; $A = LL_y]$, we have

$$j^i_d = \frac{\pi|e|\omega_c}{ALWm^*\tilde{\omega}^2}\sum_{\vec{q}_\perp,\alpha,\alpha'} q_x\langle V^2\rangle_{\vec{q}_\perp}|M_{\alpha\alpha'}(\vec{q})|^2 \times(f_{\alpha 0} - f_{\alpha' 0})\delta(E_\alpha - E_{\alpha'}) \tag{3}$$

and

$$j^p_d = \frac{2\pi|e|\omega_c}{LWm^*\tilde{\omega}^2}\sum_{\vec{q},\alpha,\alpha'} q_x|C_{\vec{q}}|^2|M_{\alpha\alpha'}(\vec{q})|^2[f_{\alpha 0}(1-f_{\alpha' 0}) + n_{\vec{q}}(f_{\alpha 0} - f_{\alpha' 0})]\delta(E_\alpha - E_{\alpha'} - \hbar\omega_{\vec{q}}). \tag{4}$$

The eigenvalues and matrix elements are given by

$$E_\alpha \equiv E_{n,k_x} = \hbar\tilde{\omega}(n+\tfrac{1}{2}) + \frac{\hbar^2 k_x^2}{2\tilde{m}} - \frac{eE_H}{\tilde{\omega}^2 m^*}\left(\hbar k_x\omega_c + \frac{eE_H}{2}\right) + E_{z0} \tag{5}$$

and

$$|M_{\alpha\alpha'}(\vec{q})|^2 = |\langle\alpha|e^{i\vec{q}\cdot\vec{r}}|\alpha'\rangle|^2 = (N!/N'!)u^{N'-N}e^{-u}[L_N^{N'-N}(u)]^2 \times F(q_z)\delta_{q_x,k_x-k'_x}, \tag{6}$$

respectively. Further, $\tilde{\omega} = (\omega_c^2 + \Omega^2)^{1/2}$, $\tilde{m} = m^*\tilde{\omega}^2/\Omega^2$, $u = [(\omega_c^2/\tilde{\omega}^2)q_x^2 + q_y^2]\tilde{\ell}^2/2$, $\tilde{\ell} = (\hbar/m^*\tilde{\omega})^{1/2}$ is the renormalized magnetic length, $L_N^{N'}(u)$ a Laguerre polynomial, and $F(q_z)$ the form factor. For $d = 0$ we have $F(q_z) = 1$; for $d$ finite and $V_z = m^*\omega_z^2 z^2/2$ we have, with $\ell_z^2 = \hbar/m^*\omega_z \ll \tilde{\ell}^2$, $F(q_z) \approx \exp(-q_z^2\ell_z^2/2)$ if $\omega_z \gg \tilde{\omega}$. For typical values $\bar{q}_z^2 \ll \ell_z^{-2}$ the result for $F(q_z)$ is almost equal to that obtained from the variational wave function $X_0(z) = z(b_0^3/2)^{1/2}\exp(-b_0 z/2)$ if $\ell_z^{-2} = b_0^2/6$, i.e., $F(q_z) = [1 + q_z^2/b_0^2]^{-3}$; in this case the average thickness is $3/b_0$. If not specified we will take $F(q_z) = 1$. Further, $f_{\alpha 0} = 1/[1 + \exp\left((E_{\alpha 0} - E_F)/k_BT\right)]$ is the Fermi-Dirac function, $E_{\alpha 0} = E_\alpha(E_H = 0)$, $E_F$ is the Fermi level, and $n_{\vec{q}}$ is the equilibrium distribution function for phonons. Notice that the initial distribution function $f_{\alpha 0}$ is a nonequilibrium one and gives a nonzero current along the channel. Thus, strictly speaking the terms "Fermi-Dirac function," $f_{\alpha 0}$, and "Fermi level," $E_F$, should not be taken at face value for $E_H \neq 0$. We emphasize that Eqs. (1)–(4) were obtained using perturbation theory and that the energy spectrum, Eq. (5), is not degenerate with respect to $k_x$. In Eq. (3) $\langle V^2\rangle_{\vec{q}_\perp}$ is the impurity

potential correlation function given by

$$\langle V(\vec{q}_\perp)V(\vec{q}'_\perp)\rangle = (2\pi)^2\delta(\vec{q}_\perp+\vec{q}'_\perp)\langle V^2\rangle_{\vec{q}_\perp}, \tag{7}$$

and $V(\vec{q}_\perp)$ is the 2D Fourier transform of the impurity potential taken in the 2DEG plane. To proceed further, we specify the kind of phonons. For the very low temperatures pertinent to the QHE, we consider only the standard acoustical (DA) and piezoelectrical (PA) phonons for which $\omega_{\vec{q}} = sq$ and $C^2_{\vec{q}} = (c'/L_xL_yL_z)q^{\pm1}$ with $c'$ a constant. If not specified we will assume a smooth confinement, $\Omega \ll |\omega_c|$, i.e., the confining potential does not affect the eigenfunctions $|\alpha\rangle$ much but it substantially changes the eigenvalues $E_\alpha$. This condition is usually fulfilled if the magnetic field is not too weak, cf. Secs. I and V. From Eqs. (1) and (2) we can express $E_H$ as a function of $E_x$, $E_H = E_H(E_x)$. Then from Eq. (2) we have

$$\begin{aligned} j_x &= \sigma^0_{xy}E_H(E_x) = \sigma^{ef}_{xx}(E_x)E_x, \\ \rho^{ef}_{xx} &= (\sigma^{ef}_{xx})^{-1} = j_d/E_H(\sigma^0_{xy})^2, \end{aligned} \tag{8}$$

for $E_x \to 0$ and $E_H \to 0$, we have linear responses in the narrow channel, i.e., $\sigma^{ef}_{xx}$ is independent of $E_x$ and $\rho^{ef}_{xx}$ is independent of $E_H$. Below we will consider only linear responses.

We will consider three different cases for $\langle V^2\rangle_{\vec{q}_\perp} \equiv \langle V^2\rangle_{q_\perp}$, $q_\perp = (q_x^2+q_y^2)^{1/2}$. When scattering centers are in the $z = 0$ 2DEG plane, with a short-range potential of a $j$ center, $U_j(\vec{r}) = U_0\delta(\vec{r}-\vec{R}_j)$, we have (i) $\langle V^2\rangle_{q_\perp} = n_IU_0^2$ and, for a Coulomb potential, (ii) $\langle V^2\rangle_{q_\perp} = (2\pi e^2/\varepsilon_0 q_\perp)^2 n_I$, where $n_I$ is the density of the scattering centers and $\varepsilon_0$ the dielectric constant; here we neglect the small difference between the dielectric constants of GaAs and $Al_xGa_{1-x}As$. For scattering due to remote impurities, at distance $z_0 > 0$ from the 2DEG plane, we have (iii) $\langle V^2\rangle_{q_\perp} = (2\pi e^2/\varepsilon_0 q_\perp)^2 n_I \exp(-2q_\perp z_0)$. In cases (ii) and (iii) we neglect the possible screening;[22] otherwise, to avoid a logarithmic divergence we change $\varepsilon_0$ to $\varepsilon_{0s} = \varepsilon_0(1+q_s/q_\perp)$ (cf. Ref. 11). Notice that for $B = 0$, the Thomas-Fermi wave vector $q_s$ should be at least smaller than the Fermi wave vector; also, the possible dependence of $q_s$ on $B$ is usually neglected.[11] Unless stated otherwise, we will assume that almost all electrons of the 2DEG are at the bottom of the $N = 0$ Landau level that coincides with $E_{\alpha 0}(k_x = 0)$. In the present study such an assumption is not crucial.

## III. IMPURITY SCATTERING IN A NARROW CHANNEL

For elastic scattering, in Eq. (3), we have $q_x(f_{\alpha 0} - f_{\alpha' 0})\delta(E_\alpha - E_{\alpha'}) \propto E_H\, q_x^2(\partial f/\partial E)_{E^0_{N,k_x}}\delta(E^0_{N,k_x} - E^0_{N',k_x-q_x})$. Then for $N = N'$, only transitions with wave vector change $q_x = 2k_x$ can be essential. Moreover, the factor $(\partial f/\partial E)_{E=E^0_{N,k_x}}$ shows that, if the temperature is sufficiently low and $\Omega$ not too small, the dissipation is mainly due to transitions with $k_x \approx \pm k_e$, i.e., *intralevel interedge* transitions. For $N \neq N'$, e.g., when the Fermi level is halfway between the two lowest Landau levels, the main contribution will be given by *interlevel intraedge* transitions between thermally populated states of these levels. The latter contribution can be essential only for large $\Omega$ and $T$.

### A. Intralevel scattering

For intralevel transitions, from Eqs. (3) and (8), we have, upon omitting the superscript $ef$ in $\rho^{ef}_{xx}$, the impurity contribution to the resistivity $\rho_{xx}$ as

$$\begin{aligned} \rho^{ia}_{xx} = \frac{2\omega_c^2}{\hbar e^2\Omega^4 W}\int_{-\infty}^{\infty}\int_{-\infty}^{\infty} dq_y dk_x \frac{k_x}{|k_x|}\langle V^2\rangle_{2k_x,q_y} \\ \times[-df(E_0(k_x))/dk_x]\exp\left(-\left[4\frac{\omega_c^2}{\tilde{\omega}^2}k_x^2+q_y^2\right]\tilde{\ell}^2\Big/2\right), \end{aligned} \tag{9}$$

where $E_0(k_x) = E_{0k_x}(E_H = 0) = \hbar\tilde{\omega}/2 + \hbar^2k_x^2/2\tilde{m} + E_{z0}$ and $W = 2\hbar\omega_c k_e/m^*\tilde{\omega}^2 = 2y_{\rm RE} \approx 2y_e$. Here $k_e = (\tilde{\omega}/\hbar\Omega)[2m^*\Delta_F]^{1/2}$ is the characteristic wave vector that represents the strength of the confinement for edge states near the intersections of the Fermi level with the $N = 0$ Landau level, $\Delta_F = (E_{F0} - \hbar\tilde{\omega}/2)$, and $E_{F0} = E_F - E_{z0}$. Further, $f(E_0(\pm k_e)) = 1/2$, $E_e = \hbar\Omega^2 k_e/|e|\omega_c$ is the characteristic electric field defining the influence of the channel boundaries on edge states,[19,21] and $y_{\rm RE}$ is the coordinate of the right edge of the channel. We will assume $\Delta_F \gg k_BT$, i.e., electrons in the $N = 0$ Landau level are degenerate. Then Eq. (9) gives

$$\rho^{ia}_{xx} = Ce^{-2(\omega_c k_e\tilde{\ell}/\tilde{\omega})^2}\int_0^\infty dq_y\langle V^2\rangle_{2k_e,q_y}e^{-q_y^2\tilde{\ell}^2/2}, \tag{10}$$

where $C = 8\omega_c^2/\hbar e^2\Omega^4 W$. Then corresponding to cases (i) and (ii) of the scattering potential we obtain, from Eq. (10),

$$\rho^{ia}_{xx} = C'e^{-2(\omega_c k_e\tilde{\ell}/\tilde{\omega})^2} = C'e^{-4\Delta_F\omega_c^2/\hbar\tilde{\omega}\Omega^2}, \tag{11}$$

and, using Ref. 23,

$$\rho^{ia}_{xx} = De^{2(\Omega k_e\tilde{\ell}/\tilde{\omega})^2}[1-\Phi(\sqrt{2}k_e\tilde{\ell})], \tag{12}$$

respectively. Here $C' = C\sqrt{\pi/2}n_IU_0^2/\tilde{\ell}$, $D = \pi^3Ce^4n_I/\varepsilon_0^2k_e$, and $\Phi(x)$ is the probability integral. Equation (10) is obtained under the linear-response condition

$$E_H \ll [\Omega(2m^*\Delta_F)^{1/2}/|e|]\min\{1;\hbar\Omega^2/8\omega_c\Delta_F\}, \tag{13}$$

assuming that $\langle V^2\rangle_{q_\perp}$, as a function of $q_x$, changes on a scale $\lesssim \tilde{\ell}^{-1}$. As can be seen, the latter condition is satisfied for both Eq. (11) and Eq. (12). For smooth confinement and $\Delta_F$ not too small, such that $4k_e\tilde{\ell} \gg 1$, Eq. (12) gives

$$\rho^{ia}_{xx} = \frac{D}{\sqrt{2\pi}k_e\tilde{\ell}}e^{-2(\omega_c k_e\tilde{\ell}/\tilde{\omega})^2} = \frac{D}{\sqrt{2\pi}k_e\tilde{\ell}}e^{-4\Delta_F\omega_c^2/\hbar\tilde{\omega}\Omega^2}. \tag{14}$$

For scattering by remote impurities, when the conditions

$2z_0/\tilde{\ell} \gg 1$ and

$$k_BT \ll \frac{\hbar\Omega\sqrt{\Delta_F}}{4z_0\sqrt{m^*\tilde{\omega}}} = \frac{\Delta_F}{2\sqrt{2}k_ez_0} \tag{15}$$

are satisfied, Eq. (10) gives

$$\rho_{xx}^{ia} = \frac{D\omega_c^2}{\tilde{\omega}^2[1+\sqrt{2\pi z_0 k_e}]}e^{-4z_0k_e}. \tag{16}$$

Condition (15) shows that $df(E_0(k_x))/dk_x$ is a sharper function of $k_x$ than $\exp(-4z_0k_x)$; thus the transition from Eq. (9) to Eq. (10) is justified. When $k_BT$ obeys the inequality opposite to (15), we obtain

$$\rho_{xx}^{ia} = \frac{D\hbar^2\Omega^2k_e}{4k_BTm^*\tilde{\omega}^2z_0}e^{-\Delta_F/k_BT}. \tag{17}$$

The regions of temperature pertinent to Eq. (17) are determined by

$$\Delta_F \gg k_BT \gg \frac{\hbar\Omega\sqrt{\Delta_F}}{4z_0\sqrt{m^*\tilde{\omega}}}. \tag{18}$$

Though the 2DEG is degenerate, we have an activated behavior of the resistivity with activation energy $\Delta_F$. Larger spacer distances $z_0$ and smoother confining potentials, i.e., smaller $\Omega$, favor the activated behavior for lower temperatures whereas a larger $\Delta_F$ widens the region of this behavior but shifts its edges to higher temperatures if $\Omega$ does not change much when $\Delta_F$ does due to the gate voltage. It seems that $\Omega$ can change when $\Delta_F$ does upon changing $B$. Indeed, the charge distribution can be changed, especially in the most important part of the sample for determining $\Omega$, i.e., in the vicinity of the edges due to even small changes of $B$ that change the Landau level degeneracy. An increase of about 30% in the area concentration of the 2DEG, in a channel with $W \approx 1000$ Å, has been observed in Ref. 24 with increasing $B$.

Notice that $\rho_{xx}^{ia}$, as given by Eqs. (11), (12), (14), and (16), is independent of temperature. For smooth confining potentials and the Fermi level not too close to the bottom of the Landau level, such that $\Delta_F/k_BT \gg 1$, $2(\omega_ck_e\tilde{\ell}/\tilde{\omega}) \approx 2k_e^2\tilde{\ell}^2 \gg 1$ or $4z_0k_e \gg 1$, we have an exponential suppression of dissipation in the narrow channel caused by *intralevel interedge* elastic scattering. However, even for smooth confining potentials, if the Fermi level is sufficiently close to the bottom of the Landau level, such that $k_e\tilde{\ell} \simeq 1$ or $k_ez_0 \simeq 1$, an exponential suppression of the dissipation due to this scattering, with typical electron coordinates $|y| \approx W/2$, is absent or too weak. In such a case $\rho_{xx}^{ia}$ can be rather large. Indeed, estimating $\rho_{xx}^{ia}$ from Eq. (14), for $B = 6.2$ T, $n_I = 10^8/\text{cm}^2$, $k_e\tilde{\ell} \approx 2$, $\Omega = 2.31 \times 10^{12}/\text{sec}$, $W \approx 2k_e\tilde{\ell}^2 \approx 400$ Å, $\varepsilon_0 \approx 12$, we obtain $\rho_{xx}^{ia} \approx (8 \times 10^3\ \Omega/\square)\ e^{-8} = 20\ \Omega/\square$, which is rather large.

In obtaining Eq. (10) from Eq. (9), we assumed that the dominant contribution to the integral comes from the factor $df_0/dk_x$, i.e., in cases (i) and (ii)

$$k_BT \ll \frac{\hbar\tilde{\omega}}{4}\frac{\Omega^2}{\omega_c^2}. \tag{19}$$

However, if $T$ is such that

$$\Delta_F \gg k_BT \gg \frac{\hbar\tilde{\omega}}{4}\frac{\Omega^2}{\omega_c^2}, \tag{20}$$

we obtain

$$\rho_{xx}^{ia} = \frac{C'\hbar\tilde{\omega}\Omega^2}{4k_BT\omega_c^2}e^{-\Delta_F/k_BT}, \tag{21}$$

for case (i) and, when $\Omega^2/\tilde{\omega}^2 \ll 1$,

$$\rho_{xx}^{ia} = \frac{D\hbar k_e\tilde{\ell}\Omega^2}{\sqrt{2\pi}k_BT\tilde{\omega}}e^{-\Delta_F/k_BT} \tag{22}$$

for case (ii). As with Eq. (17) we have again an activated behavior though the 2DEG is degenerate. This behavior is favored by smooth confining potentials, i.e., $\Omega/\tilde{\omega} \ll 1$, as is seen from Eqs. (18) and (20). Moreover, this behavior is in good agreement with that observed experimentally[1] in a channel with $W \approx 2000$ Å, $L \gtrsim 5$ $\mu$m, $B = 7.3$ T, in a GaAs/(AlGa)As heterostructure at the $\nu = 2$ minima. A more detailed comparison will be given below.

For completeness we consider the activated behavior under condition (20) when intralevel scattering occurs in the $N = 1$ Landau level. We assume $\Delta_{F1} = E_{F0} - 3\hbar\tilde{\omega}/2 < 0$, and $|\Delta_{F1}| \gg k_BT$, i.e., that the electron distribution of this level is nondegenerate. The corresponding result for $\rho_{xx}^{ia}$ is given by Eq. (9) with $\Delta_F$ replaced by $\Delta_{F1}$ in the Fermi factors and the integrand multiplied by a factor $[L_1(u)]^2$ where $u = 2k_x^2\tilde{\ell}^2\omega_c^2/\tilde{\omega}^2 + q_y^2\tilde{\ell}^2/2$. As with the $N = 0$ level under condition (20) [or (18)], the main contribution to dissipation comes from transitions between states rather close to the bottom of the level. Such transitions, involving typical electron coordinates $|y| \ll W/2$, we denote as *intracenter* transitions; of course, they are symmetric for elastic scattering.

For parabolic confinement, if condition (20) is fulfilled, we obtain, in case (i) and for $N = 1$,

$$\rho_{xx}^{ia} = \frac{C'7\hbar\tilde{\omega}\Omega^2}{32k_BT\omega_c^2}e^{\Delta_{F1}/k_BT}. \tag{23}$$

Comparing Eqs. (21) and (23) we see that for $\Delta_F < \hbar\tilde{\omega}/2$ and $|\Delta_{F1}| > \hbar\tilde{\omega}/2$, the main contribution to the intralevel dissipation comes from the $N = 0$ level. If $\Delta_F - \hbar\tilde{\omega}/2 > k_BT$ and $\Delta_{F1} < 0$, Eq. (23) gives the main contribution to the "activated" dissipation. If the spin splitting of the levels is taken into account, at the $\nu = 2$ minimum we should take the maximum $\Delta_F$ substantially smaller than $\hbar\tilde{\omega}/2$ when the spin splitting at the edges is not too small. The latter condition is favored by spin polarization that appears at the edges.[18] This corresponds to an activation energy of 3.1 meV, observed in Ref. 1, which is substantially smaller than $\hbar\omega_c/2 = 6$ meV and the activation energy 4.8 meV in a wide channel.[1] Notice also that in a wide channel an activation energy larger than $\hbar\omega_c/2$ was observed.[25]

The behavior of $\rho_{xx}^{ia}$ as a function of $\Delta_F/\hbar\tilde{\omega}$, obtained numerically from Eq. (9), is represented in Figs. 1–5. For cases (i), (ii), and (iii), it is plotted in Figs. 1, 2 and

3 for different temperatures. In each figure the frequency $\Omega$ is different. It is assumed that $B$ is constant and that changes in $\Delta_F$, due to a gate potential, do not affect $\Omega$. Here we express $\rho_{xx}^{ia}$ in units of $\tilde{\rho} = 16\pi^2 e^2 \omega_c n_I/\hbar\varepsilon_0^2\tilde{\omega}^3$. We take $B = 7.3$ T, $m^* = 0.067m_0$, $\varepsilon_0 = 12$, and $\tilde{n}_I = n_I/(10^8\ \mathrm{cm}^{-2})$. Then $\tilde{\rho} \approx 7\tilde{n}_I\ \Omega/\square$. For short-range scattering, case (i), we assume, in all figures, that $U_0 = (2\pi e^2\tilde{\ell}/\varepsilon_0)\tilde{U}_0$ with the dimensionless value $\tilde{U}_0 = 1$.

Curves 1, 2, 5, and 6, in Fig. 1, satisfy the condition (19) (here $\Delta_F \gg k_B T$) and their form is independent of $T$ since curves 1 and 5 (for $T = 0.1$ K) practically coincide with curves 2 and 6 (for $T = 1$ K), respectively. Notice that for curve 10, with $T = 1$ K, the condition (15) is not satisfied and this curve is rather different from curve 9 with $T = 0.1$ K. For all other curves in Fig. 1 the conditions (20) or (18) are satisfied and, in agreement with Eqs. (21), (22), or (17), they represent an activated behavior though the 2DEG is degenerate. In Fig. 2, the confinement is smoother than in Fig. 1, $\Omega^2/\tilde{\omega}^2 = 0.01$; we see that curves 1 and 5 deviate from curves 2 and 6, respectively, in contrast with the corresponding curves in Fig. 1. This is related with the activated behavior of curves 2 and 6 in Fig. 2 as it follows from Eqs. (20)–(22).

Comparing Fig. 3, in which the confinement is smoother ($\Omega^2/\tilde{\omega}^2 = 0.001$) than in Fig. 2, with Figs. 1 and 2, we see that for small $T$ the resistivity becomes a very sharp function of $\Delta_F/\hbar\tilde{\omega}$ if the confinement is sufficiently smooth even for scattering by the in-plane

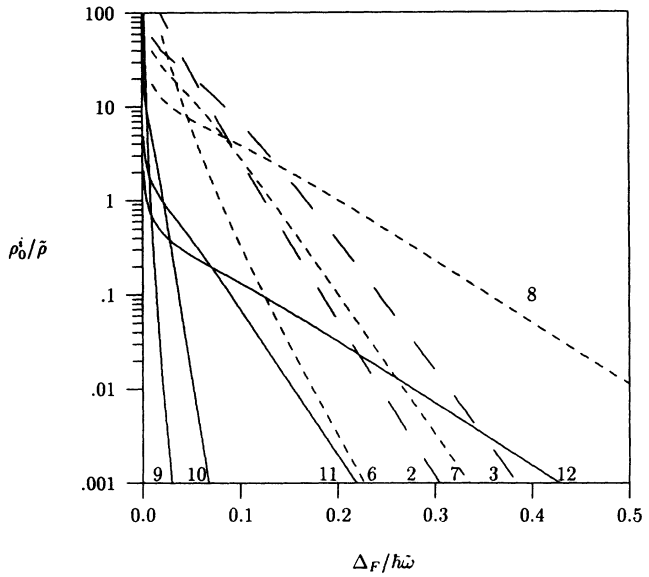


FIG. 1. Intralevel contribution to the resistivity $\rho_0^i$ from the $N = 0$ Landau level, in units of $\tilde{\rho}$, as function of the Fermi level when $\Omega^2/\tilde{\omega}^2 = 0.1$. The solid curves are for scattering by remote impurities at distance $z_0 = 290$ Å, the short-dashed curves for the in-plane Coulomb interaction, and the long-dashed curves for short-range impurities. The temperature is $T = 0.1$ K, 1 K, 4.2 K, and 10 K for the groups of curves (1,5,9), (2,6,10), (3,7,11), and (4,8,12), respectively. Curves 1, 4, and 5 follow very closely curves 2, 8, and 6, respectively, and are not shown. $\Delta_F/\hbar\tilde{\omega} = 0.0$ coincides with the bottom of the $N = 0$ Landau level.

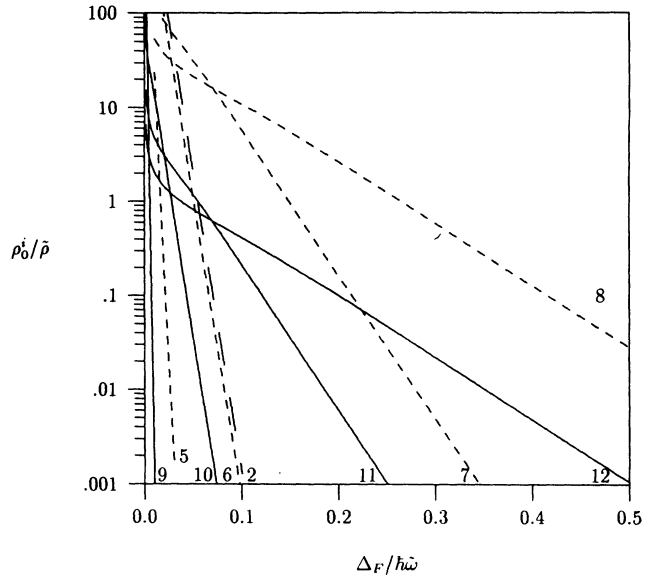


FIG. 2. Same as in Fig. 1 with $\Omega^2/\tilde{\omega}^2 = 0.01$. Curves 1, 2, 3, and 4 are close to curves 5, 6, 7, and 8, respectively. Curves 1, 3, and 4 are not shown.

Coulomb or short-range impurities (cf. curves 1, 5, and 9 in Figs. 1–3). Such dependence is related with the possibility of an activated behavior with increasing smoothness of the confining potential. Under conditions (18) and (20) with increasing $\Omega^{-1}$ we have an increase of the resistivity $\propto \Omega^{-1}$. The latter is seen from curves 8 and 12 in Figs. 1–3, i.e., for rather large $T$. The value of $\Omega$ used in Fig. 3 is close to that given in Ref. 18; $\Omega$ and the other parameters of Fig. 2 pertain to the experimental condi-

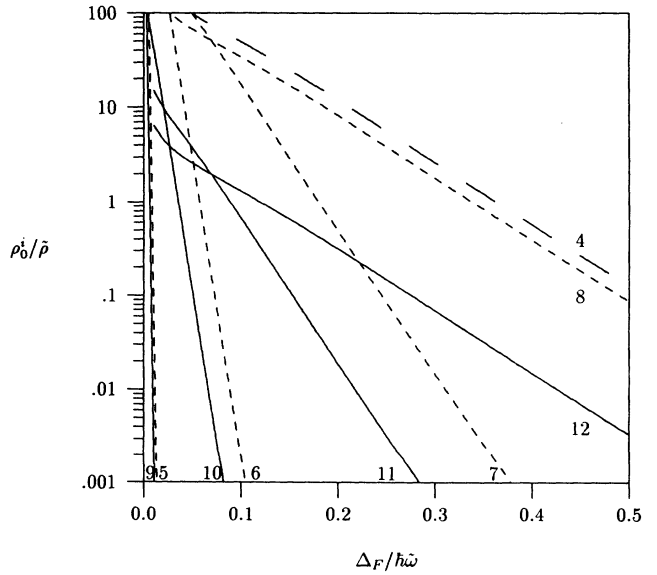


FIG. 3. Same as in Fig. 1 with $\Omega^2/\tilde{\omega}^2 = 0.001$. Curves 1, 2, and 3 almost coincide with curves 5, 6, and 7, respectively, and are not shown.

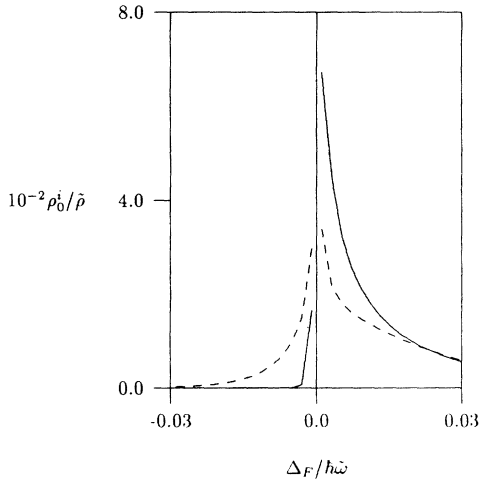


FIG. 4. The solid, dashed, and dotted curves correspond to $T = 0.1$ K, 1 K, and 4.2 K, respectively. Here $\Omega^2/\tilde{\omega}^2 = 0.1$ and $\Delta_F/\hbar\tilde{\omega} = 0$ coincides with the bottom of the $N = 0$ Landau level.

tions of Ref. 1. To avoid the logarithmic divergence of the resistivity for cases (ii) and (iii), we assume $q_s^2\tilde{\ell}^2 = 0.1$. This assumption is not crucial; indeed, from Figs. 1–3 we see that the behavior of the curves between, e.g., (i), corresponding to $q_s\tilde{\ell} \gg 1$ and (ii) is rather similar.

Figures 4 and 5 show the asymmetry in Shubnikov–de Haas oscillations and their dependence on $\Omega$ and $T$. For definiteness, in both figures we consider short-range scattering. In line with the experimental results of Refs. 26 and 17 (see also Refs. 6, 17, and 25), we have at the low-energy side of the Landau level a substantially smaller resistivity than at its high-energy side, if $T$ is not too high and $\Omega$ not too small. The latter condition is equivalent to assuming that the channel is narrow and is in agreement with the stronger asymmetry for smaller $W$ observed in Refs. 26 and 27. Notice the substantial difference in the resistivity for symmetrical values $\Delta_F$ away from the bottom of the $N = 0$ Landau level. In Fig. 4 , for $T = 0.1$ K and $T = 1$ K, this is mainly related with the temperature-independent behavior of Eq. (11) valid for $\Delta_F/\hbar\tilde{\omega} > k_BT/\hbar\tilde{\omega} \approx 4 \times 10^{-4}$ and $4 \times 10^{-3}$, respectively, and with the activated dependence similar to Eq. (23) for $\Delta_F < 0$. With increasing temperature or smoothness of the confining potential we see an activated behavior of the resistivity for both signs of $\Delta_F$. Notice that in Ref. 28 for $T = 0$ sawtooth oscillations of the resistivity were obtained that are related with the sawtooth form of the broadened density of states of a parabolic channel.

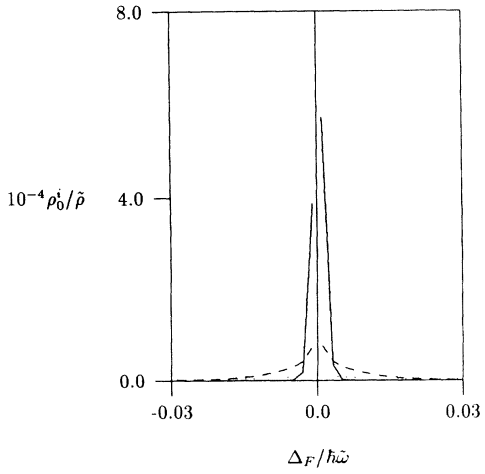


FIG. 5. Same as in Fig. 4 with $\Omega^2/\tilde{\omega}^2 = 0.001$.

### B. Interlevel and intralevel scattering

In Fig. 6 we plot the resistivity for intralevel scattering in the $N = 0$ and $N = 1$ Landau levels $\rho_T^i$ as a function of the position of the Fermi level for different $\Omega$ and $T$. For completness we also consider interlevel transitions. From Eqs. (3) and (8) their contribution to $\rho_{xx}$ is

$$\rho_{xx}^{ir} = \frac{2\omega_c^2\tilde{\ell}^4}{e^2k_BT\Omega^2\tilde{\omega}W}\int_0^\infty\int_0^\infty dq_x dq_y q_x \langle V^2\rangle_{q_\perp} \times\left(\frac{\omega_c^2}{\tilde{\omega}^2}q_x^2+q_y^2\right)\exp\left(-\left[\frac{\omega_c^2}{\tilde{\omega}^2}q_x^2+q_y^2\right]\tilde{\ell}^2/2\right) \times\frac{\exp[\hbar^2(k_0^2-q_x^2)^2/8\tilde{m}k_BTq_x^2-\tilde{\Delta}_{F1}]}{\{1+\exp[\hbar^2(k_0^2-q_x^2)^2/8\tilde{m}k_BTq_x^2-\tilde{\Delta}_{F1}]\}^2}. \quad (24)$$

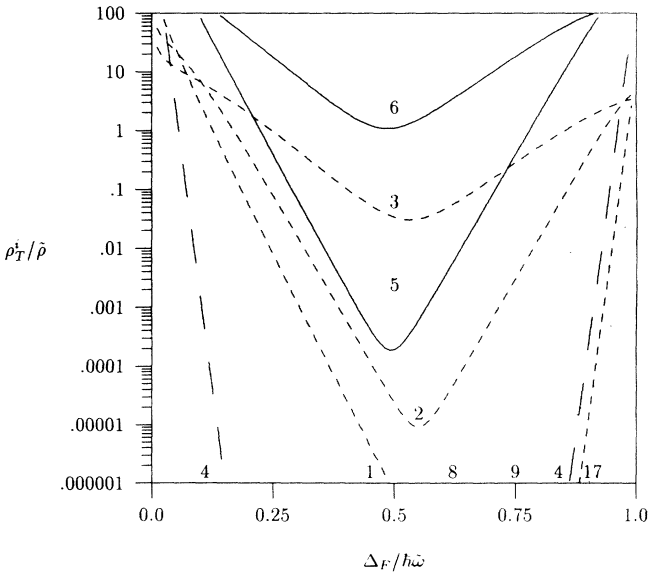


FIG. 6. Total contribution to the resistivity $\rho_T^i$ from the two lowest Landau levels, in units of $\tilde{\rho}$, as a function of the position of the Fermi level. The dotted curves 7, 8, and 9 account for interlevel transitions with $\Omega^2/\tilde{\omega}^2 = 10^{-1}$ and $\Omega^2/\tilde{\omega}^2 = 10^{-2}$, respectively. The solid, short-dashed, and long-dashed curves account for intralevel transitions from both levels with $\Omega^2/\tilde{\omega}^2 = 10^{-4}, 10^{-1}$, and $10^{-2}$, respectively. The temperature is $T = 1$ K, 4.2 K, and 10 K for the groups of curves (1, 4, 7), (2, 5, 8, 9), and (3, 6), respectively. Curve 9 has been multiplied by a factor $10^{11}$.

Here we assume that the main contribution to $\rho_{xx}^{ir} = j_d^{ir}/E_H(e^2/2\pi\hbar)^2$ comes from interlevel transitions between the $N = 0$ and $N = 1$ Landau levels. This is correct for, e.g., $\Delta_{F1} < 0$; in Eq. (24) $\tilde{\Delta}_{F1} = \Delta_{F1}/k_BT$ and $k_0^2 = 2\tilde{m}\tilde{\omega}/\hbar = 2\tilde{\ell}^{-2}\tilde{\omega}^2/\Omega^2$. Curves 7 and 8, in Fig. 6, for $\rho_{xx}^{ir}/\tilde{\rho}$ are obtained numerically from Eq. (24) for short-range impurities with $\Omega^2/\tilde{\omega}^2 = 0.1$ and $T = 1$ K and 4.2 K, respectively. Comparing curves 7 and 8 with curves 1 and 2, respectively, which describe intralevel contributions, we see that for $0.5 < \Delta_F/\hbar\tilde{\omega} < 1.0$ the interlevel contribution is at least one order-of-magnitude smaller than the intralevel one. For smaller $\Omega$ this discrepancy increases. Thus, for $\Omega^2/\tilde{\omega}^2 = 0.01$ and $T = 1$ K the intralevel contribution of curve 4 will be $10^{26}$ times larger than the interlevel one for $\Delta_F/\hbar\tilde{\omega} = 0.91$. A factor of approximately $3.3 \times 10^5$ in this value is related with the occupancy of the states pertinent to interlevel transitions [$\propto \exp(\tilde{\Delta}_{F1})$]. The remaining factor ($\approx 3 \times 10^{20}$) is too small in comparison with $\exp[(\Delta y_0^{01}/\tilde{\ell})^2/2] = \exp(k_0^2\tilde{\ell}^2) = e^{99} \approx 10^{43}$ which corresponds to the exponential factor in Eq. (5) of Ref. 3 (see also Refs. 10 and 11) if we assume $\Delta y_0^{01}$ as the separation between the two neighboring edge channels[3] at the energy corresponding to the bottom of $N = 1$ Landau level. To explain such a huge difference, we first notice that for $T \to 0$ we obtain, from Eq. (24), the same exponential factor $\exp(-k_0^2\tilde{\ell}^2) = \exp(-\omega_c^2/\Omega^2)$. However, for finite $T$, assuming $\tilde{\Delta}_{F1} \leq 0$, we obtain, in addition to the occupation factor $\propto \exp(\tilde{\Delta}_{F1})$, a factor

$$F = \exp\left\{-\left[\frac{\hbar\tilde{\omega}}{2k_BT}(1 + 4k_BT\omega_c^2/\hbar\tilde{\omega}\Omega^2)^{1/2} - 1\right]\right\}. \tag{25}$$

For $4k_BT\omega_c^2/\hbar\tilde{\omega}\Omega^2 \to 0$, $F$ tends to $e^{-\omega_c^2/\Omega^2}$. However for smooth confinement, with $\omega_c^2/\Omega^2 \gg 1$, even for rather small $T$, $F$ can be many orders-of-magnitude larger than the zero-temperature factor $e^{-\omega_c^2/\Omega^2}$. Thus, for $T = 1$ K and $\Omega^2/\tilde{\omega}^2 = 0.01$, $F$ is $\approx 10^{-29}$, i.e., much larger than $e^{-\omega_c^2/\Omega^2} \approx 10^{-43}$. This estimate of $\rho_{xx}^{ir}$, including the preexponential factor, is in good agreement with our numerical results. The optimal interlevel transitions pertinent to Eq. (25) correspond to an energy

$$E_{op}^{01} = \frac{3}{2}\hbar\tilde{\omega} + \frac{\hbar\tilde{\omega}}{4}\left(\sqrt{1+aT} + \frac{1}{\sqrt{1+aT}} - 2\right) > \tfrac{3}{2}\hbar\tilde{\omega}, \tag{26}$$

where $a = 4k_B\omega_c^2/\hbar\tilde{\omega}\Omega^2$ and $q_{x,op}^2 = k_0^2/(1+aT)^{1/2}$; it is assumed that $E_{op}^{01} < 2\hbar\tilde{\omega}$.

Comparing, in Fig. 6, curves with the same $T$ but different $\Omega$, e.g., curves 1 and 4 with 2 and 5, etc., we see that the larger $\Omega$ the more asymmetric the T dependences of $\rho_T^i$ with respect to the middle point $\Delta_F/\hbar\tilde{\omega} = 0.5$. Including interlevel contributions will obviously strengthen this behavior. This is in line with the experimental observations of Refs. 26 and 27; see also the discussion of Figs. 4 and 5. Comparing now curves for the same $\Omega$ but for different $T$, e.g., curves 1, 2, and 3, we see that with increasing $T$ the peaks of $\rho_T^i$ become more symmetric with respect to the middle point $\Delta_F/\hbar\tilde{\omega} = 0.5$. The latter is in agreement with Ref. 27.

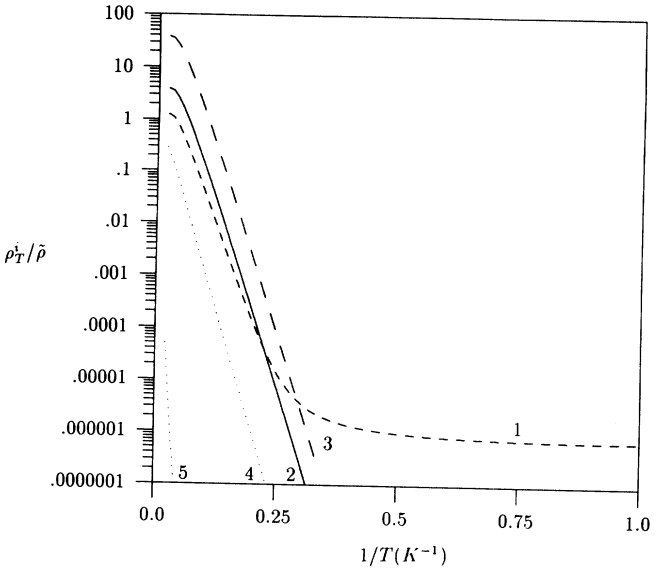


FIG. 7. Same as in Fig. 6 as a function of inverse temperature when the Fermi level is between the $N = 0$ and $N = 1$ Landau levels. The dotted curves 4 and 5 account for interlevel transitions with $\Omega^2/\tilde{\omega}^2 = 10^{-1}$ and $10^{-2}$, respectively. Curves 1, 2, and 3 account for intralevel transitions from both levels with $\Omega^2/\tilde{\omega}^2 = 10^{-1}, 10^{-2}$, and $10^{-4}$, respectively.

In Fig. 7 we plot the total contribution to the resistivity $\rho_T^i$, due to intralevel transitions in the two lowest Landau levels ($N = 0$ and $N = 1$) for scattering by short-range impurities, as a function of inverse temperature. The Fermi level is in the middle between the bottoms of these levels (curves 1, 2, and 3). Curves 4 and 5, for $\rho_{xx}^{ir}/\tilde{\rho}$, are obtained numerically from Eq. (24). Comparing curves 4 and 5, in Fig. 7, with curves representing $\rho_T^i$ we see that the interlevel contribution due to elastic scattering can be practically neglected even for $\Omega^2/\tilde{\omega}^2 = 0.1$. In line with the above treatment, curve 1 shows an activated behavior at comparatively high temperatures and a weak temperature dependence for $T \lesssim 2$ K. The regions of activated behavior in curves 2 and 3 are substantially wider, in agreement with our analytical findings. Though the qualitative behavior of curves 1 and 2 is similar to that observed in Ref. 1; for a more comprehensive comparison we must consider the electron scattering by acoustical phonons.

## IV. PHONON SCATTERING IN A NARROW CHANNEL

For completeness we consider the contribution $\rho_{xx}^{pr}$ to $\rho_{xx}$ due to interlevel transitions assisted by acoustical phonons. We also consider the intralevel contributions $\rho_{xx}^{pa}$ to $\rho_{xx}$ for conditions pertinent to the experiment of Ref. 1 using the results of Refs. 19 and 21. Due to the narrow low-mobility channel in this work, we should also treat intralevel $\rho_T^i$ and interlevel $\rho_{xx}^{ir}$ contributions to dis-

sipation due to impurities. To describe the confinement in the channel, of width $W \approx 2000$ Å, with a parabolic potential we should suppose $\Omega^2/\tilde{\omega}^2 \approx \Omega^2/\omega_c^2 \approx 0.01$, i.e., $\Omega \approx 1.9\ 10^{12}\ \mathrm{s}^{-1}$, which is more than twice as large as the $\Omega$ in Ref. 18). For conditions pertinent to Fig. 4(b) of Ref. 1, we have $\Delta_F \approx \hbar\tilde{\omega}/2$. Then for interaction with PA ($s = 2.5\times10^5$ cm/sec), and standard DA ($s = 5\times10^5$ cm/sec) phonons we have $\eta = E_e/E_s \approx 7$ and $\eta \approx 3.5$, respectively. Here $E_s = \tilde{\omega}sB/\omega_c^2$, $\eta = (\Omega/\tilde{\omega})(\hbar\tilde{\omega}/m^*s^2)^{1/2}$.

The magnitude of $\rho_{xx}^{pa}$ and its temperature dependence are very different for $\eta > 1$ and $\eta < 1$, cf. Refs. 19 and 21. For $\eta > 1$ we should have $\rho_{xx}^{pa} \propto T^3$ or $T$ for PA phonons and $\rho_{xx}^{pa} \propto T^5$ or $T$ for DA phonons when $x_T = \hbar s/\tilde{\ell}k_BT \gg 1$ or $x_T \ll 1$, respectively. For 20 K$> T >$ 4 K for both PA and DA phonons we should have $\rho_{xx}^{pa} \propto T$. Hence the above discussed activated behavior, observed in Ref. 1 for 50 K$> T >$ 7 K, cannot be associated with $\rho_{xx}^{pa}$. Such a conclusion is also supported by the estimate of the typical value $\rho_{xx}^{pa}$ for $T = 10$ K. Indeed, for PA phonons, under usually fulfilled experimental condition $\tilde{\ell}^2/\ell_z^2 \approx 1$, we have, from Eqs. (14) and (15) of Ref. 19, an expression for $j_d^p$ {differing from Eq. (20) of Ref. 19 only by a small factor $[1 + (\eta^2 - 1)\ell_z^2/\tilde{\ell}^2]^{-1/2} \approx \eta^{-1}$}, that gives for the usual parameters $\rho_{xx}^{pa} \approx 1\ \Omega/\Box$. Here we assume $c' = \hbar(eh_{14})^2/2\rho s$, $h_{14} = 1.2\times10^7$ V/cm, and $\rho = 5.31$ g/cm$^3$. Further, we neglect spin splitting and take into account a spin factor 2, which leads to twice smaller values of $\rho_{xx}$. The corresponding estimate for DA phonons [based on Eq. (24) of Ref. 19 with an additional small factor $2/\eta^3$, which appears due to the finite thickness $\ell_z$ for $\eta \gg 1$], gives $\rho_{xx}^{pa} \approx 0.5\ \Omega/\Box$. For DA phonons we assume $c' = \hbar\Xi^2/2\rho s$, $\Xi = 7$ eV. This $\rho_{xx}^{pa}$ should give a contribution to $R_{xx}$ of order $(L/W)\rho_{xx}^{pa} = 20\ \rho_{xx}^{pa} \approx 30\ \Omega/\Box$, which is still much smaller than the observed[1] $R_{xx} \approx 300\ \Omega/\Box$ for $T = 10$ K. However, it can cause a substantially slower decrease of $\rho_{xx}$, as a function of inverse temperature, in the $T$ region between 6.6 K and 20 K than that of $\rho_T^i$ in curve 2 of Fig. 7.

The interlevel transitions assisted by PA or DA phonons contribute to the dissipation at least $10^4$ times less than the intralevel ones, when a finite value of $\ell_z$ is considered, for both models of $F(q_z)$ with the reasonable value $\ell_z = \tilde{\ell}$. This is related to a rather large $\bar{q}_z$ in both cases. Moreover, until $\rho_{xx}^{pr}$ drops many orders of magnitude, for both models of $F(q_z)$ the dependences of $\rho_{xx}^{pr}$ on $T^{-1}$, after $T^{-1} = 0.02$, are very similar. Notice that the interlevel contribution, due to scattering by short-range impurities, $\rho_{xx}^{ir}$, is at least $10^4$ times smaller than the intralevel one, $\rho_{xx}^{ia}$. In Fig. 8 we plot $\rho_{xx}^{p}$, caused by both PA and DA phonons and all intralevel and interlevel transitions assisted by them, as well as $\rho_{xx}^{i}$, due to short-range impurities, as a function of inverse temperature. Here $\rho_{xx}^{i} = \rho_{xx}^{ia} + \rho_{xx}^{ir}$. Assuming $\tilde{n}_I = 20$, the unit along the $y$ axis is $\tilde{\rho} \approx 70\ \Omega/\Box$. Here due to the spin factor 2 we have a $\tilde{\rho}$ twice smaller than that of Sec. III. We also plot $\rho_{xx}^{T}$, the sum of $\rho_{xx}^{p}$ and $\rho_{xx}^{i}$. The slope of $\rho_{xx}^{T}$ in Fig. 8 is in good agreement, in the region where $\rho_{xx}^{T}$ and $\rho_{xx}^{i}$ are very close to each other, with the measured activation energy of $R_{xx} = L\rho_{xx}/W$, cf. Fig. 4(b) in Ref. 1. The same holds for the magnitude of $\rho_{xx}^{T}$. In the same

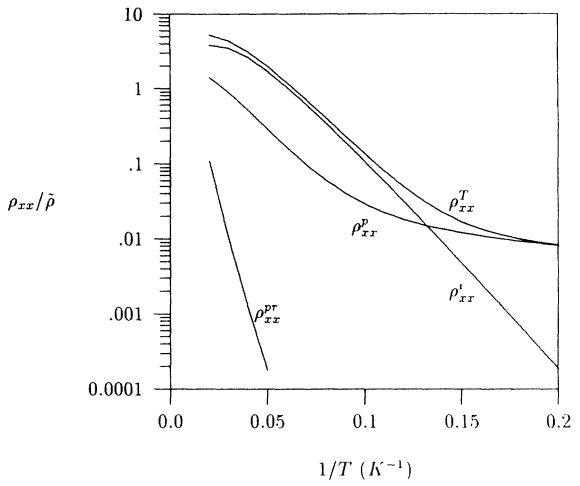


FIG. 8. Resistivity as a function of inverse temperature for scattering by impurities ($\rho_{xx}^{i}$), mainly accounted by *intralevel intracenter* transitions, and phonons ($\rho_{xx}^{p}$), mainly related with *intralevel intraedge* transitions, for $1/T \gtrsim 0.1\ \mathrm{K}^{-1}$. The total result is $\rho_{xx}^{T}$. The curve marked $\rho_{xx}^{pr}$, accounting for interlevel scattering by DA phonons, is drastically suppressed (by more than $10^4$) due to the finite thickness of the 2DEG. The result shown is multiplied by a factor $10^4$. The Fermi level is halfway between the two lowest Landau levels.

$T$ region, 50 K$> T >$ 7 K, the behavior of $\rho_{xx}^{p}$ is substantially different than the observed activated one with $\Delta_a = 3.1$ meV. For comparison we also plot the curve representing $10^4\rho_{xx}^{pr}$, related with interlevel transitions due to DA phonons which are more important here than the PA phonons. Notice that, e.g., at $1/T = 0.02\ \mathrm{K}^{-1}$ and $F(q_z) = 1$, $\rho_{xx}^{pr}$ becomes more than $10^5$ times larger than its corresponding value in Fig. 8. It is clear that in the pertinent $T$ region the main contribution to dissipation is related with intralevel center-to-edge electron transitions caused by strong impurity scattering.

## V. CONCLUDING REMARKS

One of the main results of this paper is the explanation of the activated behavior of the dissipation, observed in Ref. 1 in a low-mobility channel, by *intralevel intracenter* transitions due to impurities. This result is substantially related to the rather smooth lateral confinement in micrometer- or submicrometer-width channels, such that $W \geq 2000$ Å. We have seen with decreasing $\Omega$ the region of $T$, for which we have activated behavior, increases. Our treatment shows that elastic *intralevel interedge* electron scattering can be essential for channel widths $W < 1000$ Å, i.e., for confining potentials $V(y)$ of rather steep form. Notice that Eqs. (9)–(12) and (16), (17) are also valid for potentials that are not smooth. When the Fermi level lies in the middle between the two lowest Landau levels, we have $k_e\tilde{\ell} \sim 1$ since $\Omega \sim \omega_c$. Then Eqs. (11) and (12) lead to a very strong dissipation, due to *intralevel interedge* electron transitions. We

have also obtained a strong suppression of *intralevel intraedge* and of *interlevel intraedge* contributions (the *interlevel interedge* ones are much weaker than the latter) to dissipation, due to scattering by acoustical phonons, related with the finite thickness $d$ of the 2DEG. This result is obtained for $\eta = E_e/E_s \gg 1$, i.e., for the condition pertinent to the experiment of Ref. 1 for which a smooth confinement, i.e., small $\Omega \ll \omega_c$, is well justified.

In line with experimental results[26,27] (see also Refs. 6, 17, and 25) we have obtained the asymmetry in the Shubnikov–de Haas oscillations and its dependence on $\Omega$ and $T$. In particular, at the low-energy side of the Landau level we have a substantially smaller resistivity than at its high-energy side, if the temperature is not too high and the confinement not too smooth. The asymmetry of the resistivity for symmetric values $\Delta_F$, with respect to the bottom of the Landau level, is mainly related to its insensitivity to temperature, cf. Eq. (11) valid for $\Delta_F/\hbar\tilde{\omega} > k_BT/\hbar\tilde{\omega}$. It's also related to an activated behavior similar to that of Eq. (23), for $\Delta_F$ of the same modulus but of opposite sign. Thus, this finite temperature result complements that of Ref. 28 for $T = 0$ where the calculated saw-tooth oscillations of the resistivity reflected the saw-tooth form of the broadened density of states of a parabolic channel.

We have considered only the linear-response regime. This is sufficient for elastic scattering in a parabolic channel if $j_x$ or $E_H$ is small. Hence, from Eq. (13) and for parameters pertinent to conditions of the experiment,[1] we obtain $|e|E_H\tilde{\ell} \ll \hbar\omega_c(\Omega/\omega_c)^3$ and $E_H \ll 10$ V/cm. Notice that for $E_H = 1$ V/cm and other pertinent conditions we obtain $j_x \approx 0.01$ A/m. This is close to the highest current densities used in Ref. 1 without any influence of $j_x$ on the measurement.

## ACKNOWLEDGMENTS

The work was supported by NSERC Grant No. OGPIN028 (P.V., O.B.) and by the Fund for Fundamental Investigations of Ukraine GKNT (O.B.).

[1] A. M. Chang, G. Timp, T. Y. Chang, J. E. Cunnigham, P. M. Mankievich, R. E. Behringer, and R. E. Howard, Solid State Commun. **67**, 769 (1988).
[2] M. Buttiker, Phys. Rev. B **38**, 9375 (1988).
[3] T. Martin and S. Feng, Phys. Rev. Lett. **64**, 1971 (1990).
[4] B. J. van Wees, E. M. M. Willems, L. P. Kouwenhoven, C. J. P. M. Harmans, J. G. Williamson, C. T. Foxon, and J. J. Harris, Phys. Rev. B **39**, 8066 (1989).
[5] B. W. Alphenaar, P. L. McEuen, R. G. Wheeler, and R. N. Sacks, Phys. Rev. Lett. **64**, 677 (1990).
[6] P. L. McEuen, A. Szafer, C. A. Richter, B. W. Alphenaar, J. K. Jain, A. D. Stone, R. G. Wheeler, and R. N. Sacks, Phys. Rev. Lett. **64**, 2062 (1990).
[7] P. C. van Son, F. W. de Vries, and T. M. Klapwijk, Phys. Rev. B **43**, 6764 (1991).
[8] S. Komiyama, H. Hirai, M. Ohsawa, H. Matsuda, S. Sasa, and T. Fujii, in *Proceedings of 20th International Conference on the Physics of Semiconductors, Thessaloniki, 1990*, edited by E. M. Anastassakis and J. D. Joannopoulos (World Scientific, Singapore, 1990), p. 1150.
[9] S. Komiyama, H. Hirai, M. Ohsawa, H. Matsuda, S. Sasa, and T. Fujii, Phys. Rev. B **45**, 11 085 (1992).
[10] J. J. Palacios and C. Tejedor, Phys. Rev. B **44**, 8157 (1991).
[11] S. M. Badalian, Y. B. Levinson, and D. L. Maslov, Pis'ma Zh. Eksp. Teor. Fiz. **53**, 595 (1991) [JETP Lett. **53**, 619 (1991)].
[12] R. J. F. van Haren, F. A. P. Blom, W. de Lange, and J. H. Wolter, Phys. Rev. B **47**, 15 700 (1993).
[13] K. von Klitzing, Physica B **184**, 1 (1993).
[14] P. F. Fontein, P. Hendriks, F. A. Blom, J. H. Wolter, L. J. Gilling, and C. W. J. Beenakker, Surf. Sci. **263**, 91 (1992).
[15] D. J. Thouless, Phys. Rev. Lett. **71**, 1879 (1993).
[16] K. K. Choi, D. C. Tsui, and K. Alavi, Appl. Phys. Lett. **50**, 110 (1987).
[17] B. E. Kane, D. C. Tsui, and G. Weimann, Phys. Rev. Lett. **59**, 1353 (1987).
[18] G. Muller, D. Weiss, A. V. Khaetskii, K. von Klitzing, S. Koch, H. Nickel, W. Schlapp, and R. Losch, Phys. Rev. B **45**, 3932 (1992).
[19] O. G. Balev and P. Vasilopoulos, Phys. Rev. B **47**, 16 410 (1993).
[20] D. B. Chklovskii, B. I. Shklovskii, and L. I. Glazman, Phys. Rev. B **46**, 4026 (1992).
[21] O. G. Balev, P. Vasilopoulos, and E. V. Mozdor, Phys. Rev. B **50**, 8706 (1994).
[22] G. A. Toombs, F. W. Sheard, D. Nelson, and L. J. Challis, Solid State Commun. **64**, 577 (1987).
[23] G. Gradshteyn and I. M. Ryzhik, *Tables of Integrals, Series, and Products* (Academic, New York, 1965).
[24] G. Timp, A. M. Chang, P. Mankiewich, G. Bobinger, J. E. Cunningham, T. Y. Chang, and R. E. Howard, Phys. Rev. Lett. **59**, 732 (1987).
[25] K. von Klitzing, G. Ebert, N. Leinmichel, H. Obloch, G. Dorda, and G. Weinmann, *The 17th International Conference on the Physics of Semiconductors* (Springer-Verlag, New York, 1985), p. 271.
[26] H. Z. Zheng, K. K. Choi, and D. C. Tsui, Phys. Rev. Lett. **55**, 1144 (1985).
[27] R. J. Haug, K. von Klitzing, and K. Ploog, Phys. Rev. B **35**, 5933 (1987).
[28] P. Vasilopoulos, Superlatt. Microstruct. **5**, 583 (1989).